

CONTROL OF LASER RADIATION PARAMETERS

PACS numbers: 42.15.Dp; 07.60.Ly
DOI: 10.1070/QE2001v031n10ABEH002071

Measurements of small wave-front distortions using a three-wave lateral shearing interferometer

V I Sokolov

***Abstract*. The solution of the parabolic equation for radiation diffracted from a periodic hexagonal structure is analysed theoretically. It is shown that diffraction does not prevent high-precision measurements of wave-front distortions using a three-beam lateral shearing interferometer. The proposed measuring technique is based on the recording of interference-pattern distortions at arbitrary distances from a beam replicator. The results of numerical calculations supporting this technique are presented. The optical quality of an etalon plate is measured in an aperture of diameter 12 cm with a high degree of precision. By considering the example of a large-aperture KDP crystal, it is shown that the application of this method makes it possible to synthesise from individual measurements the wave front in an aperture considerably larger than the test beam aperture.**

Keywords: *wave-front distortions, beam replicator, three-wave shearing interferometer, phase reconstruction.*

1. Introduction

High-precision measurements of the quality of optical elements are essential for many applications associated with the creation of diffraction-limited laser beams. Along with interference methods, the Shack – Hartmann methods [1, 2] which are more convenient for practical applications are used for this purpose. When periodic structures are employed, measurements can be made using the Talbot effect [3, 4] or the method of three-wave lateral shearing interferometer [5, 6], which was developed quite recently. In the latter case, an analysis of the transport equation for radiation intensity [7, 8] made it possible to propose an algorithm of wave-front reconstruction, which is based on the Fourier transform and makes it possible to determine simultaneously the wave front derivatives in chosen directions over the entire cross section of the beam.

Note that while deriving formulas for these derivatives, displacements were considered for which diffraction could be neglected. To improve the sensitivity of the method upon an increase in the displacement of the plane of image recording, it was also proposed to filter radiation in the Fourier plane to eliminate the effect of diffraction. This idea was developed further in paper [9], where a phase plate of hexagonal configuration was used as a wave-front replicator. The possibility of compensating optical distortions introduced by the optical system of measurements itself during the recording of intensity distribution with and without the optical object under study in the same plane away from the replicator was also noted in Ref. [5]. This property is important for measuring the quality of optical elements.

In this work, we consider the possibility of using a three-wave lateral shearing interferometer for high-precision measurements of the optical element quality on the basis of a theoretical analysis of the solution of the parabolic equation for radiation diffracted from a periodic hexagonal structure.

V I Sokolov State Scientific Center of the Russian Federation 'Troitsk Institute of Innovation and Fusion Research', 142190 Troitsk, Moscow oblast, Russia; e-mail: sokolov@triniti.ru; vicsok@rambler.ru

Received 26 June 2001
Kvantovaya Elektronika **31** (10) 891 – 896 (2001)
Translated by Ram Wadhwa

2. Derivation of the formula for calculating transverse gradients of the wave front in chosen directions

Consider the parabolic equation describing the propagation of a monochromatic beam along the z axis:

$$2ik\frac{\partial \boldsymbol{A}(\boldsymbol{r},z)}{\partial z}+\Delta \boldsymbol{A}(\boldsymbol{r},z)=0, \tag{1}$$

where $\boldsymbol{A}(\boldsymbol{r},z)$ is the complex amplitude of the field, $\boldsymbol{r}$ is the radius vector in a plane perpendicular to the direction of propagation, and k is the modulus of the wave vector. Following Ref. [5], we write the expression for the field amplitude in the plane of a hexagonal wave-front replicator ($z=0$) in the form

$$A(\boldsymbol{r},0)=\sum_{j=1}^{3}A(\boldsymbol{r})\exp\left[\mathrm{i}\boldsymbol{k}_j\boldsymbol{r}+\mathrm{i}W(\boldsymbol{r})\right], \tag{2}$$

where $\boldsymbol{k}_j$ is the wave vector determining the direction of propagation of the replicated reference beam with the wave front $W(\boldsymbol{r})$. We will solve Eqn (1) with the boundary condition (2). Applying the two-dimensional Fourier transform to both sides of Eqn (1) and solving the obtained differential equation, we obtain the following expression for the Fourier components of the field amplitude at a distance z from the replicator:

$$\hat{\mathrm{F}}\left[A(\boldsymbol{r},z)\right]=\hat{\mathrm{F}}\left[A(\boldsymbol{r},0)\right]\exp\left(-\frac{\mathrm{i}}{2k}|\boldsymbol{f}_{\boldsymbol{r}}|^2z\right), \tag{3}$$

where $\boldsymbol{f}_{\boldsymbol{r}}$ is the radius vector in the Fourier plane. Applying

the inverse Fourier transform to Eqn (3), we obtain the solution for the field in the case of a displacement along the z axis in the form of a convolution of the initial field distribution with the function $\alpha(\boldsymbol{r}, z)$:

$$A(\boldsymbol{r}, z) = A(\boldsymbol{r}, 0) * \alpha(\boldsymbol{r}, z), \tag{4}$$

where

$$\alpha(\boldsymbol{r}, z) = \hat{\mathrm{F}}^{-1}\Big[\exp\Big(-\frac{\mathrm{i}}{2k}|\boldsymbol{f}_r|^2 z\Big)\Big].$$

Substituting expression (2) for the initial field distribution into Eqn (4) and taking into account the linearity of the convolution operation, we obtain the following expression for the field amplitude:

$$A(\boldsymbol{r}, z) = \sum_{j=1}^{3} \exp(\mathrm{i}\boldsymbol{k}_j\boldsymbol{r})\Big\{\int A(\boldsymbol{r}-\boldsymbol{r}')\exp\big[-\mathrm{i}\boldsymbol{k}_j\boldsymbol{r}' + \mathrm{i}W(\boldsymbol{r}-\boldsymbol{r}')\big] \times \alpha(\boldsymbol{r}', z)\mathrm{d}\boldsymbol{r}'\Big\}. \tag{5}$$

The radiation intensity is determined by the product of complex conjugate fields (5) and has the form

$$I_0(\boldsymbol{r}, z) = \sum_{j=1,\,m=1}^{3} \exp\big[\mathrm{i}(\boldsymbol{k}_j - \boldsymbol{k}_m)\boldsymbol{r}\big] G_{jm}(\boldsymbol{r}, z), \tag{6}$$

where

$$G_{jm}(\boldsymbol{r}, z) = \gamma(\boldsymbol{r}, \boldsymbol{k}_j, z)\gamma^*(\boldsymbol{r}, \boldsymbol{k}_m, z);$$

$$\gamma(\boldsymbol{r}, \boldsymbol{k}_j, z) = \int A(\boldsymbol{r}-\boldsymbol{r}')\exp\big[-\mathrm{i}\boldsymbol{k}_j\boldsymbol{r}' + \mathrm{i}W(\boldsymbol{r}-\boldsymbol{r}')\big]\alpha(\boldsymbol{r}', z)\mathrm{d}\boldsymbol{r}'.$$

We represent the function $G_{jm}(\boldsymbol{r}, z)$ in the form

$$G_{jm}(\boldsymbol{r}, z) = g_{jm}(\boldsymbol{r}, z)\exp\big[\mathrm{i}\psi_{jm}(\boldsymbol{r}, z)\big], \tag{7}$$

where $g_{jm}(\boldsymbol{r}, z) = |G_{jm}(\boldsymbol{r}, z)|$. Because $G_{mj}(\boldsymbol{r}, z) = G^*_{jm}(\boldsymbol{r}, z)$, we have $g_{mj}(\boldsymbol{r}, z) = g_{jm}(\boldsymbol{r}, z)$ and $\psi_{mj}(\boldsymbol{r}, z) = -\psi_{jm}(\boldsymbol{r}, z)$. Taking into account Eq. (7), we can write the radiation intensity in the form

$$I_0(\boldsymbol{r}, z) = \sum_{j=1,\,m=1}^{3} g_{jm}(\boldsymbol{r}, z)\exp\big\{\mathrm{i}\big[(\boldsymbol{k}_j - \boldsymbol{k}_m)\boldsymbol{r} + \psi_{jm}(\boldsymbol{r}, z)\big]\big\}. \tag{8}$$

Actually, Eqn (8) reflects the fact that the radiation intensity distribution in the z plane is a superposition of interference patterns obtained from the radiation replicas propagating in the direction of wave vectors $\boldsymbol{k}_j$, $\boldsymbol{k}_m$ and $\psi_{jm}(\boldsymbol{r}, z)$ is the difference in the wave fronts of the corresponding radiation replicas.

We assume that formulas (6) and (8) determine the distribution of radiation intensity in the absence of the object being tested and that phase distortions introduced by it are described by the function $\varphi(\boldsymbol{r})$. In this case, the amplitude of distortions of the intensity distribution pattern is proportional to the displacement z from the replicator plane and is determined by transverse gradients of the intensity distribution and of phase distortions. Indeed, the difference between the interference patterns in the plane of observation is

$$\delta I_0(\boldsymbol{r}, z) = \nabla I_0(\boldsymbol{r}, z)\mathrm{d}\boldsymbol{r},$$

and, since $\mathrm{d}\boldsymbol{r} = \nabla\varphi(\boldsymbol{r})z$, we have

$$\delta I_0(\boldsymbol{r}, z) = \nabla I_0(\boldsymbol{r}, z)\nabla\varphi(\boldsymbol{r})z. \tag{9}$$

It should be noted that the Talbot interferometry is based precisely on this formula and on the fact of a periodic reproduction of the intensity distribution of radiation that has passed through the periodic structure at distances multiple to the Talbot length L_T. For a one-dimensional grating, we have $L_{\mathrm{T}0} = 2d^2/\lambda$ (where d is the grating period and λ is the radiation wavelength) [4], while for a two-dimensional hexagonal grating used by us here, we have $L_\mathrm{T} = (3/4)L_{\mathrm{T}0}$ [10].

Thus, in the presence of the object being tested, the intensity distribution has the form

$$I_1(\boldsymbol{r}, z) = I_0(\boldsymbol{r}, z) + \delta I_0(\boldsymbol{r}, z),$$

or, taking into account formulas (6) and (9),

$$I_1(\boldsymbol{r}, z) = I_0(\boldsymbol{r}, z) + z\nabla\varphi(\boldsymbol{r}) \sum_{j=1,\,m=1}^{3} \exp\big[\mathrm{i}(\boldsymbol{k}_j - \boldsymbol{k}_m)\boldsymbol{r}\big] \times \big[\mathrm{i}(\boldsymbol{k}_j - \boldsymbol{k}_m)G_{jm}(\boldsymbol{r}, z) + \nabla G_{jm}(\boldsymbol{r}, z)\big]. \tag{10}$$

It follows from formula (10) that in the Fourier plane, the intensity has seven components (one central and six side components). If we select one of the side components with the help of a filtering function T_{jm} (e.g., equal to unity inside the circle whose radius is equal to half the separation between harmonics and equals zero on the remaining plane) and carry out the inverse Fourier transform, we can determine the gradient $\partial\varphi(\boldsymbol{r})/\partial\boldsymbol{u}_{jm}$ of phase distortions introduced by the object in the direction of the vector

$$\boldsymbol{u}_{jm} = \frac{1}{|\boldsymbol{k}_j - \boldsymbol{k}_m|}(\boldsymbol{k}_j - \boldsymbol{k}_m).$$

For this purpose, we carry out the following transformation:

$$\hat{\mathrm{F}}^{-1}\big[T_{jm}\hat{\mathrm{F}}[I_1(\boldsymbol{r}, z)]\big] = \hat{\mathrm{F}}^{-1}\big[T_{jm}\hat{\mathrm{F}}[I_0(\boldsymbol{r}, z)]\big]\Phi_{jm}(\boldsymbol{r}, z), \tag{11}$$

where

$$\Phi_{jm}(\boldsymbol{r}, z) = 1 + \Big\{\frac{\nabla g_{jm}(\boldsymbol{r}, z)}{g_{jm}(\boldsymbol{r}, z)} + \mathrm{i}\big[(\boldsymbol{k}_j - \boldsymbol{k}_m) + \nabla\psi_{jm}(\boldsymbol{r}, z)\big]\Big\}\nabla\varphi(\boldsymbol{r})z. \tag{12}$$

While deriving formula (11), we have used the equality

$$\hat{\mathrm{F}}^{-1}\big[T_{jm}\hat{\mathrm{F}}[I_0(\boldsymbol{r}, z)]\big] = \exp[\mathrm{i}(\boldsymbol{k}_j - \boldsymbol{k}_m)\boldsymbol{r}]G_{jm}(\boldsymbol{r}, z).$$

The imaginary component of expression (12) contains the quantity $(\boldsymbol{k}_j - \boldsymbol{k}_m)\nabla\varphi(\boldsymbol{r})$ proportional to the gradient $\partial\varphi(\boldsymbol{r})/\partial\boldsymbol{u}_{jm}$ of phase distortions in the direction of the vector $\boldsymbol{u}_{jm}$, as well as the product of the gradients $\nabla\psi_{jm}(\boldsymbol{r}, z)\nabla\varphi(\boldsymbol{r})$.

The condition for the applicability of this method in the case of a reference beam with the wave front $W(\boldsymbol{r})$ is the relation $|\nabla W(\boldsymbol{r})| < \frac{1}{2}|\boldsymbol{k}_j - \boldsymbol{k}_m|$; i.e., the divergence of the

reference beam must be smaller than the beam divergence determined by the period of the 2D grating. It was noted above that the function $\psi_{jm}(\boldsymbol{r}, z)$ is the difference in the wave fronts of the radiation replicas propagating in directions $\boldsymbol{k}_j$ and $\boldsymbol{k}_m$. These wave fronts are displaced relative to each other by $\sim|\boldsymbol{k}_j - \boldsymbol{k}_m|z/k$ in the transverse plane (as a rule, the value of this displacement is much smaller than the test beam aperture). Consequently, $|\nabla\psi_{jm}(\boldsymbol{r}, z)| \ll |\nabla W(\boldsymbol{r})|$ and, hence, we can disregard the second term in the brackets in expression (12).

Thus, the expression for the derivative of phase distortions in the direction of vector $\boldsymbol{u}_{jm}$, which are introduced by the object under study, can be written in the form

$$\frac{\partial\varphi(\boldsymbol{r})}{\partial\boldsymbol{u}_{jm}} = \frac{1}{|\boldsymbol{k}_j - \boldsymbol{k}_m|z}\,\mathrm{Im}\left[\Phi_{jm}(\boldsymbol{r}, z)\right], \tag{13}$$

where the function

$$\Phi_{jm}(\boldsymbol{r}, z) = \frac{\hat{\mathrm{F}}^{-1}\left[T_{jm}\hat{\mathrm{F}}[I_1(\boldsymbol{r}, z)]\right]}{\hat{\mathrm{F}}^{-1}\left[T_{jm}\hat{\mathrm{F}}[I_0(\boldsymbol{r}, z)]\right]} \tag{14}$$

is determined from the filtered Fourier spectra of radiation intensity in the displaced plane in the absence and in the presence of the object. It can easily be proved that the intensity $I_1(\boldsymbol{r}, z)$ in expression (14) can be replaced by the quantity $\delta I_0(\boldsymbol{r}, z)$, i.e., the difference between the interference patterns in the plane of observation.

For an axially symmetric distribution of the reference beam intensity, expression (13) is absolutely exact. Indeed, consider in greater detail the function

$$G_{jm}(\boldsymbol{r}, z) = \int\int B(\boldsymbol{r}, \boldsymbol{r}', z)B^*(\boldsymbol{r}, \boldsymbol{r}'', z) \times \exp(-\mathrm{i}\boldsymbol{k}_j\boldsymbol{r}' + \mathrm{i}\boldsymbol{k}_m\boldsymbol{r}'')\mathrm{d}\boldsymbol{r}'\mathrm{d}\boldsymbol{r}'',$$

where $B(\boldsymbol{r}, \boldsymbol{r}', z) = A(\boldsymbol{r} - \boldsymbol{r}')\exp[\mathrm{i}W(\boldsymbol{r} - \boldsymbol{r}')]\alpha(\boldsymbol{r}', z)$. For an axially symmetric beam, we have $B(\boldsymbol{r}, \boldsymbol{r}', z) = B(-\boldsymbol{r}, -\boldsymbol{r}', z)$ and the function $G_{jm}(\boldsymbol{r}, z)$ is purely real because the integrand becomes complex conjugate upon the replacement of $\boldsymbol{r}'$, $\boldsymbol{r}''$ by $-\boldsymbol{r}'$, $-\boldsymbol{r}''$. In this case, $\psi_{jm}(\boldsymbol{r}, z) = 0$ and expressions (11) and (12) lead to (13) and (14).

Note also that the above derivations of the formulas are valid for any other periodic structure, e.g., for a quadratic structure typical of a four-wave shearing interferometer.

Having determined the directional derivatives of the wave front, we determine the derivatives in the rectangular system of coordinates, after which their Fourier transform is used for calculating the Fourier transform of the wave front. Applying the inverse Fourier transform, we obtain the reconstructed wave front. The details of this analysis can be found in Ref. [11].

We can also propose a method for measuring the radiation wave front from the difference in the interference patterns using the same expressions (13) and (14). First, two images are recorded in the plane of the replicator and in the displaced plane. Then, the interference pattern for the propagation of radiation with a plane wave front between the replicator plane and the displaced plane is calculated and the wave front for which the calculated interference pattern is used as a reference is reconstructed.

Thus, the method proposed here is a modification of the Talbot interferometry because the information on wave-front distortions can be obtained not from the deformation of the intensity distribution over the Talbot length, but from the deformation of the interference pattern in the plane of observation at an arbitrary distance from the wave-front replicator. This is possible because the information on the wave front is contained in the Fourier spectra of radiation intensity, which can be determined theoretically for any displacement.

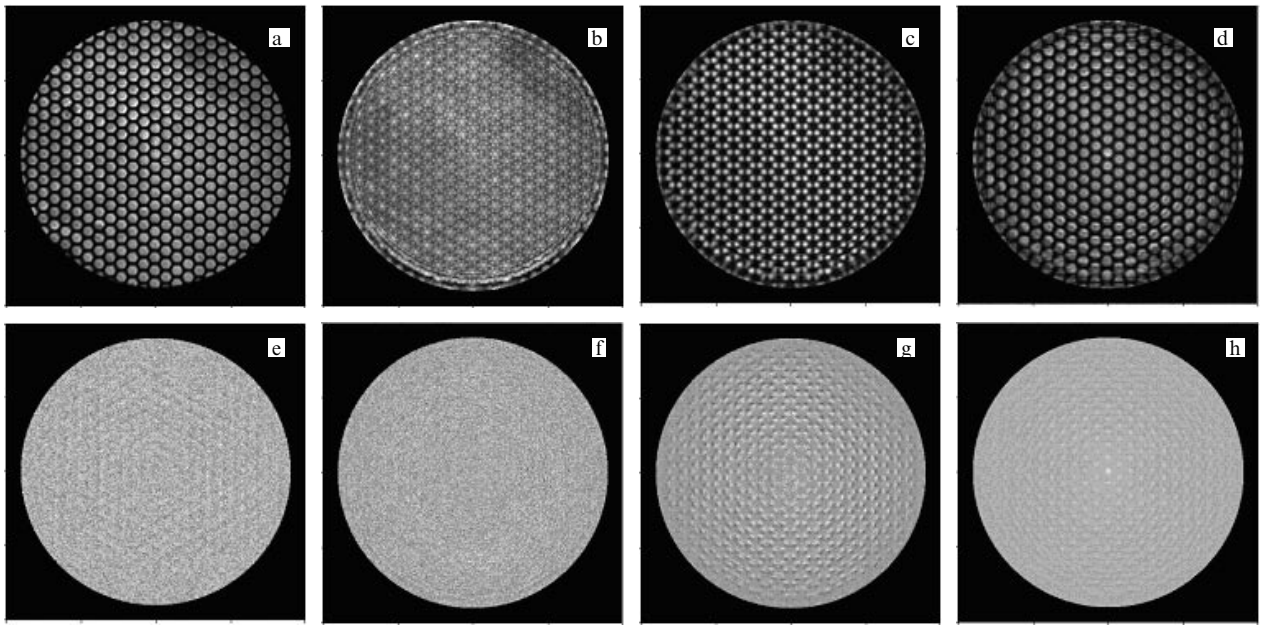

Figure 1. Radiation-intensity distributions measured in the replicator plane (a) and calculated at distance of 3 (b), 6 (c), and 12 cm (d) from the replicator as well as the differences in interference patterns calculated by introducing phase distortions with the amplitude 0.2λ at distances of 1 (e), 3 (f), 6 (g), and 12 cm (h) from the replicator for the reference beam divergence equal to two diffraction limits.

In actual practice, a limitation associated with an insufficient resolution of the setup or the computational mesh appears in experiments or in calculations. If the calculated or measured intensity-distribution pattern is not clear (the computational mesh spacing is not small enough or the resolution of the CCD camera is inadequate), the Fourier transform will be noisy and the wave-front reconstruction will be inaccurate. Nevertheless, high-precision measurements of wave-front distortions introduced by the object under study are possible for a wide range of distances not exceeding the Talbot length. As an illustration, consider the results of model calculations on the reconstruction of phase distortions of the object, which were made for various displacements from the replicator. The calculations were carried out on a net with 512×512 meshes. We used the experimentally measured intensity distribution as the initial image of the replicator in the reference plane. The phase of reference beam and phase distortions of the object (with the amplitude 0.2λ) were set analytically. The beam intensities in displaced planes were calculated by the spectral method using Fourier transforms [12]. These distributions were superimposed by a 5% random noise and the algorithm of reconstruction of phase distortions was then employed.

Figs. 1b–d show the calculated interference patterns for various distances from the replicator. The differences in the interference patterns for certain distances from the replicator (the distance 12 cm in this case is virtually equal to the Talbot length) are presented in Figs. 1e–h. These patterns display model phase distortions and a noticeable change in the contrast within the Talbot length. Fig. 2 shows the results of wave-front reconstruction demonstrating a decrease in the root-mean-square error in the reconstruction of phase distortions for more contrast beam intensity distributions.

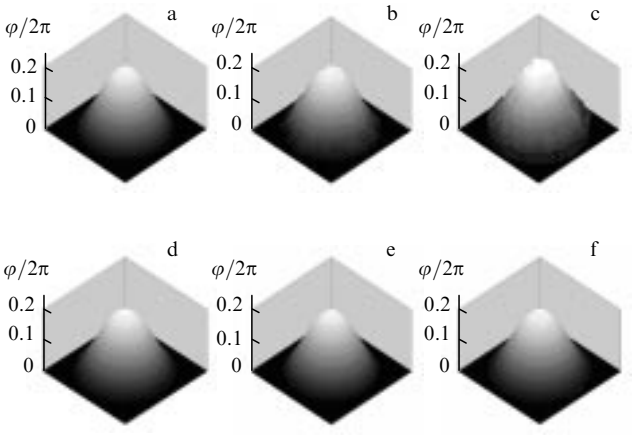

Figure 2. Specified wave-front distortion (a) and its theoretical reconstructions corresponding to the difference interference patterns presented in Fig. 1 for distances 1 (b), 3 (c), 9 (d), and 12 cm (e) from the replicator and standard deviations from the wave front equal to 0.0072λ (b), 0.027λ (c), 0.005λ (d), 0.0024λ (e), and 0.0076λ (f).

3. Test bench and results of measurements

The optical diagram of the test bench is shown in Fig. 3. The radiation from a He–Ne laser (*1*) is collimated by microscope (*2*) and lens (*4*) into a beam with an aperture $\varnothing$ 12 cm and a divergence not exceeding two diffraction limits. The optical element under study was installed on a translation table permitting its positioning in a plane orthogonal to the direction of beam propagation. The image of the output end of the optical element (*5*) under study is transferred on the wave-front replicator (9) with the help of mirrors (*6*) and a sevenfold reduction telescope (*7*). The replicator was a hexagonal diaphragm grating with a period of 850 μm and a working aperture up to 22 mm.

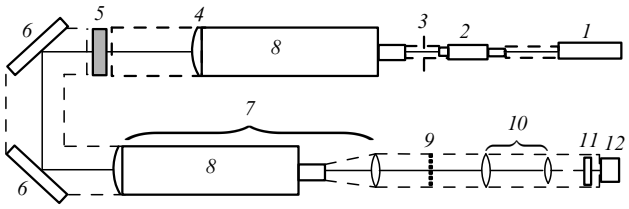

Figure 3. Optical scheme of the bench for optical element quality measurements: (*1*) He–Ne laser; (*2*) microscope; (*3*) filtering diaphragm of diameter 200 μm; (*4*) lens; (*5*) optical element under study, mounted on a translation table; (*6*) deflecting mirrors; (*7*) telescope; (*8*) tubes from an OSK-2 optical bench without eyepieces with an objective having the focal length 1.6 m; (*9*) hexagonal beam replicator; (*10*) fourfold-reduction telescope with a focal length of the objective of 1 m; (*11*) optical filter; (*12*) CCD camera from an LBA–PC 400 complex. Dashed lines show the tubes covering the optical scheme of the test bench.

In turn, the image of the replicator located in the focal plane of telescope (*10*) is transferred with an approximately fourfold reduction on the CCD camera, which can be displaced with a high degree of precision along the direction of beam propagation. Note that in order to eliminate vibrations and to be able to reproduce reliably the results of measurements, the optical setup was installed on special optical tables (whose total weight was ~ 7.5 t) in a hall with a massive foundation. The entire optical setup was encased in paper pipes to reduce the effect of air convection during measurements. The He–Ne laser and the power supply of the CCD camera were switched on for heating at least 30 min prior to the measurements.

Images were recorded using a Spiricon LBA PC-400 system with the COHU-6400 CCD camera coupled with a Pentium-200 PC and allowing an averaging over a definite number of frames $N \leqslant 256$ upon observation of cw radiation. This makes it possible to reduce the random noise by a factor of $\sqrt{N}$ (e.g., in the case of a heat source like an incandescent lamp). However, in our case with a laser source and with averaging over 256 frames, the noise was reduced only by a factor of 2 or 3. The results of individual measurements were stored in a 512×480 elements matrix file, which was enlarged to 512×512 elements by using an appropriate program so that a fast Fourier transform could be used. The wave front was reconstructed using a Pentium III PC (450 MHz) with the help of the above-described algorithm. The possible tilt of the wave front was eliminated at the end of the algorithm using the method of least squares.

Experimental measurements were made upon the longitudinal displacement of the CCD camera over a distance of 56 mm (about half the Talbot length), on which the distribution pattern changes significantly (cf. the distribution patterns presented in Figs 1a and 1c). The precision of measurements was determined using the following simple method: the image was measured several times in a displaced plane without the object. The wave front was then recon-

structed under the assumption that any frame is a reference frame. In the absence of noise, the result is obvious: an absolutely plane wave front must be reconstructed at the output (in actual practice, it differs from the plane front). However, the standard deviation σ calculated from the beam aperture does not exceed 0.03λ.

As an illustration, Fig. 4a shows a typical distribution pattern obtained during experimental determination of possible errors. Fig. 4b shows the results of reconstruction of phase distortions introduced by the etalon plate into the beam. The difference between the maximum and minimum distortions of the wave front amounts to 0.18λ and is in good agreement with the results of measurements using a Zygo Mark II interferometer (approximately 0.2λ).

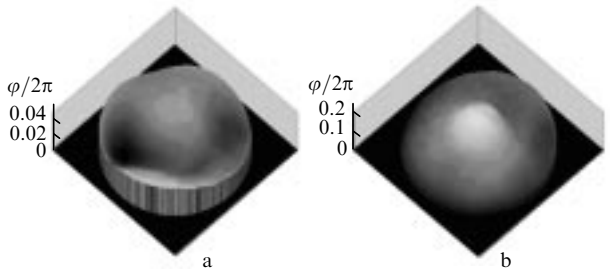

Figure 4. (a) Typical distribution pattern obtained during the experimental determination of the precision of measurements (the standard deviation from a plane wave front does not exceed 0.03λ) and (b) the results of measurements and reconstruction of optical distortions introduced by the etalon plane in the beam (the difference between the maximum and minimum deviations is 0.18λ).

The application of this method makes it possible to synthesise the wave front in an aperture considerably larger than the test beam aperture from the results of individual measurements (nine in our case). Let us demonstrate this for the measurements of the optical quality of a KDP crystal with an aperture of 24×24 cm. In the absence of the crystal, the reference image of the replicator was recorded in a displaced plane. Then the crystal was mounted on the translation table and the images of the replicator were recorded successively according to the diagram presented in Fig. 5a. Bold lines depict circles of diameter 12 cm, intended for positioning of the test beam, while thin lines are the circles in which the wave front was reconstructed without eliminating its tilt.

Then, individual wave fronts are superimposed using a special program according to the scheme presented in Fig. 5b. Because the wave fronts are determined to within a constant, the differences in wave fronts are calculated at nodal points (see Fig. 5b) and the constants for wave fronts minimising the discontinuities at the boundaries are determined from the phase continuity condition. After this, the procedure for eliminating the tilt of the synthesised wave front as a whole is employed. The results of such a reconstruction in an aperture of size 20×20 cm are presented in Fig. 6. In two cases (Figs 6b and 6d), the crystal was rotated through 90° to demonstrate the features of phase distortions inherent in the object. In order to facilitate the comparison, the wave front presented in Fig. 6d was programmed to turn through 90°. The coincidence of the wave fronts was satisfactory with a standard deviation below 0.05λ.

4. Conclusions

Thus, high-precision measurements of wave-front distortions can be made using a three-wave lateral shearing interferometer. Diffraction in this case does not prevent precise measurements and there is no need for harmonic filtration in the Fourier plane. The analysis of the solution

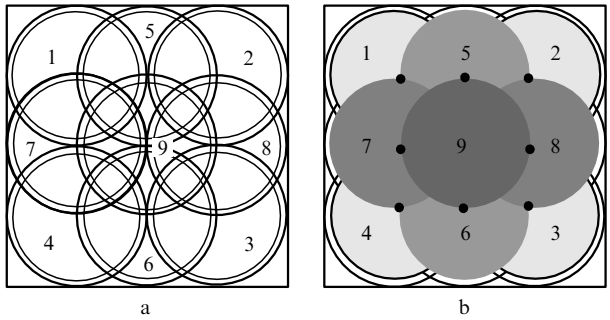

Figure 5. (a) Image of the screen for positioning of the test radiation beam and (b) the diagram of superposition of wave fronts in the synthesised aperture with nodal points (●). The numbers indicate the sequence of measurements and superposition of wave fronts upon the reconstruction of the synthesised wave front.

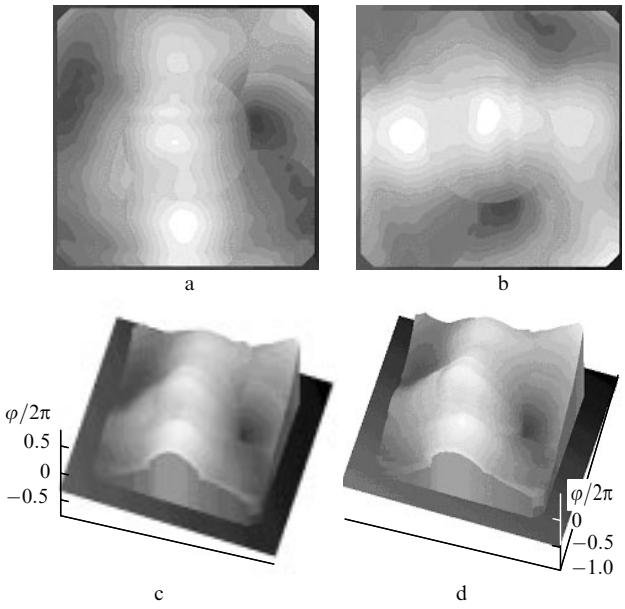

Figure 6. Results of the reconstruction of a synthesised wave front of a KDP crystal in a 20×20 cm aperture in contour (a, b) and three-dimensional (c, d) views with a direct position of the crystal (a, c) and for its rotations through 90° in a plane orthogonal to the direction of test beam (b, d) (the peak-to-valley difference is 1.04λ).

of the parabolic equation for radiation diffracted from a hexagonal periodic structure led to the expression for calculating the wave front gradients in chosen directions, which is similar to that proposed in Ref. [5] and is valid for displacements over arbitrary distances. In fact, a three-wave interferometer for the Talbot interferometry for arbitrary distances from the wave front replicator is used in the proposed method. This is possible since the information on wave-front distortions can be extracted from the Fourier spectra of radiation intensity, which can be determined theoretically for an arbitrary displacement, as confirmed by numerical calculations.

The possibility of precise measurements of the optical quality of etalon optical plates in an aperture of diameter 12 cm is demonstrated. The radiation intensity distribution was recorded at a distance approximately equal to half the Talbot length from the replicator. The experimental root-mean-square error did not exceed 0.03λ. The measurements of the optical quality of a large-aperture KDP crystal with an aperture of 24×24 cm revealed that the application of the given method makes it possible to synthesise the wave front in an aperture of size 20×20 cm, which is much larger than the aperture of the test beam, from the results of individual measurements.

Acknowledgements. The author is grateful to V G Kuznetsov for his assistance in carrying out the experiments and to R V Smirnov for useful discussions.

References

1. Shack R V, Platt B C *J. Opt. Soc. Am.* **61** 656 (1971)
2. Koch J A, Presta R W, Sacks R A, Zacharias B A, Bliss E S, et al. *Appl. Opt.* **39** 4540 (2000)
3. Talbot F *Phil. Mag.* **9** 401 (1836)
4. Rayleigh R J *Phil. Mag. J. Sci. (5th ser.)* **9** 196 (1881)
5. Primot J *Appl. Opt.* **32** 6242 (1993)
6. Primot J, Sogno L *J. Opt. Soc. Am.* **85** 2679 (1995)
7. Teague M R *J. Opt. Soc. Am.* **72** 1199 (1982)
8. Streibl N *Opt. Commun.* **49** 6 (1984)
9. Primot J, Sogno L, Fracasso B, Heggarty K *Opt. Eng.* **36** 901 (1997)
10. Kandidov V P, Kondrat'ev A V, Surovitskii M B *Kvantovaya Elektron.* **25** 712 (1998) [*Quantum Electron.* **28** 692 (1998)]
11. Nugumanov A M, Smirnov R V, Sokolov V I *Kvantovaya Elektron.* **30** 435 (2000) [*Quantum Electron.* **30** 435 (2000)]
12. Elkin N N, Napartovich A P *Prikladnaya optika lazerov* (Applied Laser Optics) (Moscow: TsNIIatominform, 1988).